

Revista Mexicana de Astronomía y Astrofísica

Revista Mexicana de Astronomía y Astrofísica
Universidad Nacional Autónoma de México
rmaa@astroscu.unam.mx
ISSN (Versión impresa): 0185-1101
MÉXICO

2002
F. Bacciotti
DIAGNOSTIC DETERMINATION OF IONIZATION AND DENSITY IN STELLAR JETS
FROM LINE RATIOS
Revista Mexicana de Astronomía y Astrofísica, volumen 013
Universidad Nacional Autónoma de México
Distrito Federal, México
pp. 8-15

Red de Revistas Científicas de América Latina y el Caribe, España y Portugal

Universidad Autónoma del Estado de México

reDalyC
LA BIBLIOTECA CIENTÍFICA EN LÍNEA
<http://redalyc.uaemex.mx>

DIAGNOSTIC DETERMINATION OF IONIZATION AND DENSITY IN STELLAR JETS FROM LINE RATIOS

F. Bacciotti^{1,2}

RESUMEN

Jets supersónicos Herbig-Haro (HH) altamente colimados han sido reconocidos como elementos esenciales del proceso de formación estelar. Muestran un espectro dominado por líneas ópticas rojas como son [O I] λ 6300, H α , [N II] λ 6583, [S II] $\lambda\lambda$ 6716,6731. Aunque se acepte generalmente que líneas como éstas se producen en gas excitado por ondas de choque moderadas, las condiciones físicas detalladas del plasma sigue siendo objeto de debate. A través de observaciones, la densidad de electrones n_e se encuentra fácilmente del doblete [S II], pero otros parámetros cruciales, como la fracción de ionización del hidrógeno x_e (y con ello la densidad total, n_H), y la temperatura promedio del flujo, no se conocen bien. Recientemente, hemos elaborado una nueva técnica de diagnóstico espectroscópico que nos ha permitido encontrar estas cantidades de manera independiente de los modelos. Empezando con una estimación de n_e , el procedimiento combina los cocientes [O I]/[N II] y [S II]/[O I] para determinar la fracción de ionización y una estimación de la temperatura de electrones. Luego se puede determinar la pérdida media de masa y la tasa de transferencia de momentum en el chorro. El procedimiento se ha aplicado primeramente a un conjunto de jets HH y flujos bipolares de estrellas T Tauri, usando espectros de resolución mediana tomados desde la Tierra. La reciente automatización del procedimiento nos ha permitido analizar imágenes y espectros de alta resolución angular ($\leq 0''.1$) tomados con el *Telescopio Espacial Hubble*. De éstos hemos derivado los primeros mapas temporales detallados de las propiedades físicas tanto a lo largo como a través del flujo. Las investigaciones han identificado una serie de características interesantes, entre las cuales encontramos que los jets HH están solamente parcialmente ionizados ($0.02 < x_e < 0.4$), y que la fracción de ionización aparentemente se incrementa rápidamente cerca de la fuente, para alcanzar una planicie y luego disminuir suavemente a lo largo del chorro.

ABSTRACT

Highly collimated, supersonic Herbig-Haro (HH) jets have been recognized as an essential element of the star formation process. They show an emission-line spectrum dominated by optical red lines as [O I] λ 6300, H α , [N II] λ 6583, [S II] $\lambda\lambda$ 6716,6731. Although it is widely accepted that such lines are produced in a gas excited by mild shocks, the detailed physical conditions of the plasma are still under debate. Observationally, the electron density n_e is easily found from the [S II] doublet, but other crucial physical parameters, as the hydrogen ionization fraction x_e (and hence the total density, n_H), and the average temperature of the flow, are poorly known. Recently, we have elaborated a new spectroscopic diagnostic technique that has allowed us to find these quantities in a model-independent way. Starting with an estimate of n_e , the procedure combines the ratios [O I]/[N II] and [S II]/[O I] to derive the ionization fraction and an estimate of the electron temperature. One can then derive the average mass loss and momentum transfer rates in the jet beam. The procedure has been applied first to a sample of HH jets and bipolar outflows from T Tauri Stars, using moderate spatial resolution spectra taken from ground. The recent automation of the procedure has allowed us to analyze large high angular resolution ($\leq 0''.1$) images and spectra taken with the *Hubble Space Telescope*. From the latter we have derived for the first time detailed maps of the physical properties both along and across the flow. These investigations have identified a number of interesting features, among which the fact that HH jets are only partially ionized ($0.02 < x_e < 0.4$), and that the ionization fraction appears to increase rapidly close to the source, to reach a plateau, and then decline gently along the beam.

Key Words: HERBIG-HARO OBJECTS — ISM: JETS AND OUTFLOWS — LINE: FORMATION

1. INTRODUCTION

Herbig-Haro (HH) jets, i.e., the highly collimated atomic mass flows observed in association with many

Young Stellar Objects (YSOs) have now been studied for two decades (e.g., Ray 1996), but some of their features remain almost unknown. An important parameter for any jet model is the hydrogen total density n_H of the flow. For example, an estimate of its value is needed to determine the jet mass loss

¹Dublin Institute for Advanced Studies, Ireland.

²Osservatorio Astrofisico di Arcetri, Italy.

and momentum transfer rates, which are useful constraints on theories of both the accretion/ejection engine (Königl & Pudritz 2000; Shu et al. 2000) and the possible interaction with the environment (Downes & Ray 1999). To know n_{H} is also essential to calculate the emission associated with a given scenario, and to provide an appropriate pre-shock density for radiative shock models (Hartigan, Morse, & Raymond 1994). Many other examples can be found, but despite its crucial importance, the total density has been rarely determined in HH jets, since it cannot be measured directly. Most of the proposed methods to find the hydrogen density are either affected by reddening and/or are largely model dependent (see, e.g., Hartigan et al. 1994). On the contrary, the electron density, n_{e} , is easily found from the ratio of the [S II] $\lambda\lambda 6716, 6731$ lines. Thus, if we have a model-independent method to find the *hydrogen ionization fraction*, x_{e} , in the flows, we could give a reliable “observational” estimate of the local total density simply as $n_{\text{H}} = n_{\text{e}}/x_{\text{e}}$.

This presentation is dedicated to the description of a such a method (called hereinafter *BE technique*), that allows one to determine the local ionization (and the electron temperature T_{e}) directly from the relative fluxes of the brightest lines in a jet, without making any assumption about the heating mechanism. The current improved version of the procedure, which was originally proposed in Bacciotti, Chiuderi, & Oliva (1995), is described in detail in Bacciotti & Eisloffel (1999) (hereinafter BE99). Here I will recapitulate its basic features, with special attention to the underlying assumptions and to the validity range (§ 2). In § 3, I will briefly list a number of general results obtained from the analysis of ground-based spectra, while the following part (§ 4) will be devoted to the illustration of new results derived from the analysis of high angular resolution (0'1) narrowband images and spectra taken with instruments on-board the *Hubble Space Telescope (HST)*. The derived 1D and 2D maps of the relevant physical quantities offer potentially very interesting insights into the physical conditions of the acceleration and collimation regions at the base of the jets (§ 5).

2. THE ‘BE TECHNIQUE’

The diagnostic procedure uses ratios of easily observed lines in HH jets. In fact, it requires as inputs the values of (i) the [S II] $\lambda 6716$ /[S II] $\lambda 6731$ ratio, to estimate the electron density n_{e} ; (ii) the [O I] ($\lambda 6300 + \lambda 6363$)/[N II] ($\lambda 6548 + \lambda 6583$) ratio, which is basically dependent only on the ionization fraction, x_{e} ; and (iii) [S II] ($\lambda 6716 +$

$\lambda 6731$)/[O I] ($\lambda 6300 + \lambda 6363$), which is much more sensitive to the electron temperature T_{e} .

The analysis is limited to the initial ‘beam’ of stellar jets, i.e., the filamentary knotty structure extending from the source to a distance of about 0.1 pc. We assume that the medium is in atomic form, and optically thin in the relevant lines. In most of our analyses the abundances adopted were $\text{N}/\text{H} = 1.1 \times 10^{-4}$, $\text{O}/\text{H} = 6.0 \times 10^{-4}$ and $\text{S}/\text{H} = 1.6 \times 10^{-5}$. The atomic upper levels relevant for the observed transitions are populated by collisions with electrons, but *we do not make any assumptions on the agent heating the gas*. Since, however, the gas in the jet beam is usually found to be of low excitation, we consider only the first ionization stage for S, O and N. Moreover, we assume that photoionization is not important in the examined region. The latter position is justified by the fact that the source is usually a low mass star with little production of ionizing radiation, and the weak ($v_{\text{shock}} \leq 35 \text{ km s}^{-1}$) shocks that may be present in the beam as miniature working surfaces (Ray et al. 1996) do not produce large amounts of UV radiation (Hollenbach & McKee 1989). In such conditions, the emissivity $\epsilon_{Z^i, \nu}$ in any forbidden line emitted at frequency ν by an atom Z in the stage of ionization i can be written as:

$$\epsilon_{Z^i, \nu} = A_{\nu} h\nu x_{\text{e}} n_{\text{H}}^2 \left(\frac{Z}{\text{H}}\right) \left(\frac{Z^i}{Z}\right) \left[\frac{n_{\text{u}}}{n(Z^i)}\right], \quad (1)$$

where A_{ν} is the transition probability, Z/H is the abundance of the element, Z^i/Z the fractional ionic abundance, and $n_{\text{u}}/n(Z^i)$ is the fractional population of the upper level. In our case, the latter is regulated by the set of equations of statistical equilibrium, that we solve numerically as a function of n_{e} and T_{e} using public routines coded by A. Raga.

The ‘kernel’ of the BE technique, however, is the functional dependence of the ionization state of the considered species from the basic physical quantities, as illustrated in the following. In low-excitation nebulae, S can be considered to be all singly ionized. For oxygen and nitrogen the ionization state is regulated by (mainly) charge exchange reactions with hydrogen, by collisional ionization and by radiative and dielectronic recombination. Now, the ionization state of O and N can be described by equilibrium rate equations (see below), but the same does not hold for H, since its ionization fraction in the rarefied high speed jet gas can be largely out of thermal equilibrium. This is justified by the fact that the typical recombination time for hydrogen is longer by one to two orders of magnitude than the charac-

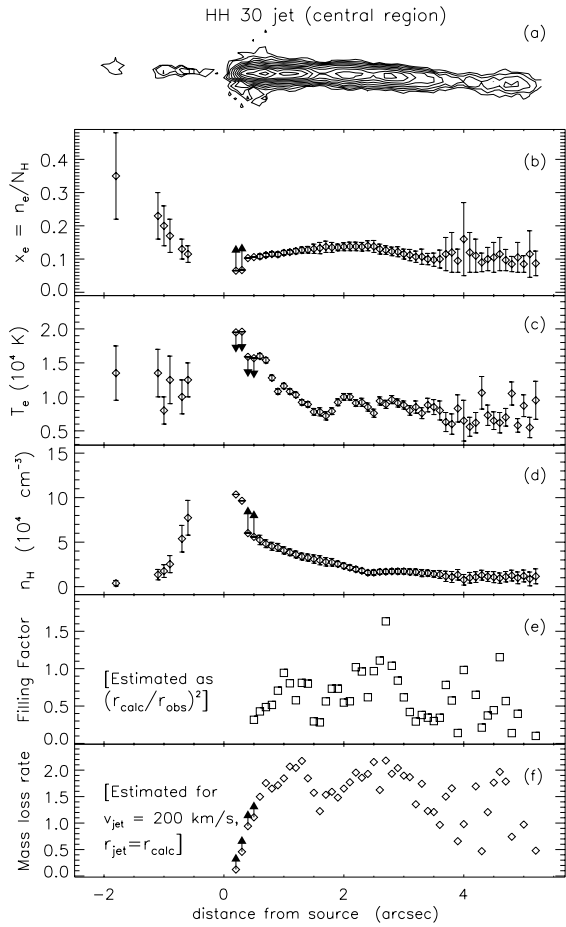


Fig. 1. Physical conditions along the HH 30 jet, at *HST* resolution. (a) [S II] *HST* image. (b) Ionization fraction. (c) Temperature. (d) Total density $n_H = n_e/x_e$. (e) Filling factor estimate (see text). (f) \dot{M} in units of $10^{-9} M_\odot \text{yr}^{-1}$.

teristic timescales for internal dynamics (Bacciotti et al. 1995). This situation, in which a ‘flash’ hydrogen ionization is created and suddenly ‘frozen’ in the plasma, can also occur in other rapidly expanding diffuse objects, as planetary nebulae and nova ejecta. On the other hand, the processes involving O and N are faster than H recombination, thus these species can still be considered in ionization equilibrium with H. The above discussion formally leads to the fact that the fractional populations of O^+ and N^+ are strongly coupled with x_e , as shown in equation (2); x_e , however, must be left as a free parameter in the calculation.

$$\frac{\text{O}^+}{\text{O}^0}, \frac{\text{N}^+}{\text{N}^0} = \frac{(C_{\text{O,N}} + \delta_{\text{O,N}})x_e}{(\alpha_{\text{O,N}} - \delta'_{\text{O,N}})x_e + \delta'_{\text{O,N}}}. \quad (2)$$

In the above expression, $C_{\text{O,N}}$ are the collisional ionization rates, $\alpha_{\text{O,N}}$ are the direct plus dielectronic recombination rates, $\delta_{\text{O,N}}$ and $\delta'_{\text{O,N}}$ are the direct and inverse charge exchange ionization rates, respectively. Since the implemented rates depend on T_e only (see Raga, Mellema, & Lundqvist 1997), the ionization state of O and N can be expressed as a function of x_e and T_e . Thus, the intensity ratio of any two of the observed lines is a *known* function of n_e , x_e and T_e . By comparing observed ratios with those calculated by means of eqs. 1 and 2, it is possible to retrieve the values of the above parameters, and hence to calculate the hydrogen density n_H in the emitting gas. The inversion can be performed either graphically (see, e.g., Fig. 1 of BE99) or numerically (Bacciotti et al. 2001), if one deals with huge sets of data (see § 4).

Accuracy and limits The sensitivity of our diagnostic results to the adopted parameters (e.g., abundances, atomic parameters, etc.) and to the observational uncertainties (extinction, critical densities, etc.) has been analyzed in BE99, Bacciotti, Eisloffel, & Ray (1999), and Lavalley (2000). These studies show that the accuracy is generally very good for the estimates of n_e ($\leq 3\%$), far from the [S II] critical density ($\sim 2 \times 10^4 \text{cm}^{-3}$), while for T_e and x_e the accuracy is about 15–20% and 20–30%, respectively. Lavalley (2000), using independent routines, also investigates the reliability of the predictions of the BE technique as the conditions of applicability progressively fail to hold.

In its first version the diagnostic procedure used ratios involving $\text{H}\alpha$ (Bacciotti et al. 1995; Bacciotti, Hirth, & Natta 1996), since this is line very bright in HH jets and the ratio [S II]/ $\text{H}\alpha$ has been historically considered a good indicator of the gas excitation. The use of $\text{H}\alpha$, however, can be misleading in this case since in a mild shock it can be produced both by collisional excitation and by recombination, in regions not physically homogeneous (Hartigan, priv. comm., see BE99, Bally & Reipurth 2002). The forbidden lines, on the contrary, come from regions of similar intermediate temperature and ionization, thus they provide unequivocal determinations. Using the forbidden lines only, our results are in good agreement with shock diagnostics (BE99, Hartigan et al. 1994). We stress, however, that oxygen and nitrogen may not be in ionization equilibrium immediately after a shock front or in the presence of turbulent boundary layers (Lavalley 2000; Binette et al. 1999). It must also be considered that while the ionization fraction has a smooth behaviour in a post-shock cooling layer, the temperature drops rapidly

by two orders of magnitude. Thus, the retrieved T_e is only an average value, unless one can work with very high angular resolution. We also point out that one must be cautious when deriving estimates of the average mass density of the nebula from the derived *local* n_H . To obtain a reliable estimate of the average mass density, one should take into account the possible effects of shock compression and/or filling factors (see Bacciotti et al. 1999 for a discussion).

The main limit to the present version of the BE technique, however, actually resides in the fact that photoionization has not been included yet. Although this is not essential for the study of the beams of HH jets (see BE99) the inclusion of photoionization is our first priority among the future developments, together with the treatment of higher ionization states of the considered elements. This will allow us to analyze the physical conditions in the highly excited terminal bow-shocks, as well as to examine objects of different nature, as peculiar regions of planetary nebulae or the recently discovered irradiated jets (see Bally & Reipurth (2002)).

3. RESULTS: I. GROUND-BASED SPECTRA

We first analyzed a sample of well-known Herbig-Haro jets, (RW Aur jet, HH 34, HH 46/47, HH 24G, HH 24C/E, HL Tau and Th 28 jets) using moderate resolution (1–1''8) spectra taken from the ground (Bacciotti et al. 1996; Bacciotti & Eisloffel 1999). We found a number of general features, summarized as follows.

1. The gas is partially ionized, with $0.02 < x_e < 0.4$, with x_e being higher for more excited and lighter jets, and in regions of violent interaction with the environment. The ionization fraction is generally observed to slowly decrease along the beam. An exception is the Th 28 jet, for which x_e first rapidly rises to reach a plateau, and then slowly decreases.

2. The average electron temperature varies typically between 9000 and 12,000 K, consistent with mild shock excitation.

3. x_e is generally found to be much higher than that produced in coronal equilibrium, and/or by the weak shocks appropriate to the observed temperature and velocities. As mentioned in the previous section, the initial ionization may be produced in the acceleration/collimation region and then be 'frozen' into the plasma, which is rapidly expanding at its base; then the gas would slowly recombine as it travels along the beam. Such a scenario would explain the 'anomaly' of the Th 28 jet.

4. Often the decrease of x_e follows a well-defined recombination curve; internal shocks are likely to be

too weak to appreciably contribute to the ionization. In other cases there are re-ionization events along the beam (see BE99): here x_e increases suddenly, and is then observed to slowly decay downstream of the ionization jump. The latter evidence would be better explained in terms of interaction with the jet surroundings then by models of internal working surfaces.

5. The local total hydrogen density n_H ranges between about 10^3 and a few 10^4 cm^{-3} . Taking into account shock compression and filling factors may reduce the estimated average density (see § 2).

6. With no density correction, the mass outflow rate varies between 10^{-9} and $10^{-7} M_\odot \text{ yr}^{-1}$. The border regions of the jet, however, may contain a significant portion of the mass but be too cold to be observable in the forbidden lines (see Bacciotti et al. 1999; Shang et al. 2001).

These early analyses indicated that something weird and potentially interesting happens very close to the source, maybe in connection with the yet unclear accelerating mechanism. In order to shed light on this aspect, one needs to investigate in detail the very first arcseconds of the outflow, at much higher angular resolution. With this idea in mind, we recently applied the BE technique to *HST* data of HH jets in Taurus. The next section illustrates the results obtained.

4. RESULTS: II. *HST* DATA

We first examined the case of the HH 30 jet, using a combination of narrowband [S II], [O I] and H α images obtained with *HST*/WFPC2 and two long-slit spectra taken from the ground. In this way we have derived the variation of x_e , T_e and n_H (all integrated over the transverse jet section) along the first 5'' of the jet (i.e., $\sim 10^{16}$ cm) with a spatial resolution of 0''.1 (Bacciotti et al. 1999). The main results are illustrated in Fig. 1. As with the other jets we have examined, HH 30 appears to be weakly ionized, with $x_e < 0.15$ in the main jet (panel b). Contrary to what is observed at lower resolution, however, we see here that the ionization fraction *increases* up to 0.140 in the first two arcseconds, reaches a plateau, and then after 2''.4 it slowly decreases down to 0.04 at about 12''. At the same time, T_e rapidly falls from $\sim 2 \times 10^4$ K to 10^4 K in less than 1'', then it decays more slowly to about 6×10^3 K at 5'' (panel c). It is noteworthy that local peaks in T_e are observed at the location of the knots, but no such increase is seen in x_e and n_H : if the knots indeed correspond to weak shocks, a reduced localized compression might be due to the presence of a transverse magnetic field in

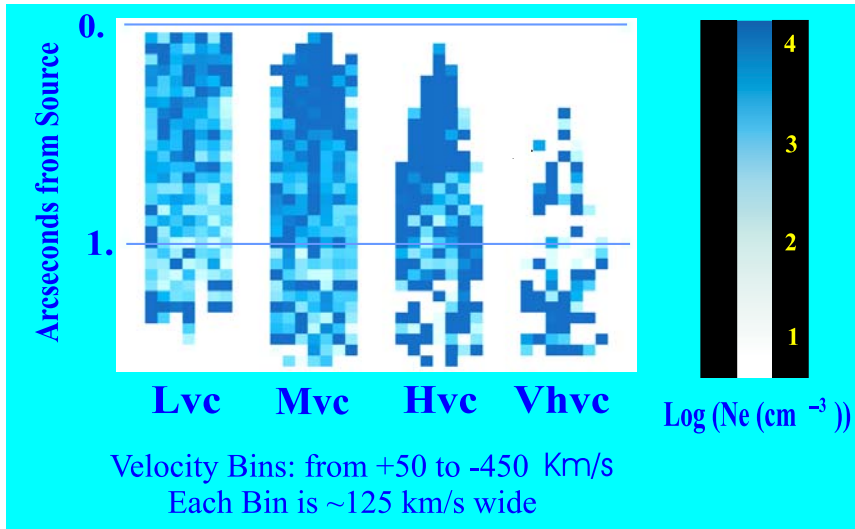


Fig. 2. 2D high angular resolution map of the electron density n_e in the first 1.5'' of the DG Tau jet, in four distinct velocity intervals.

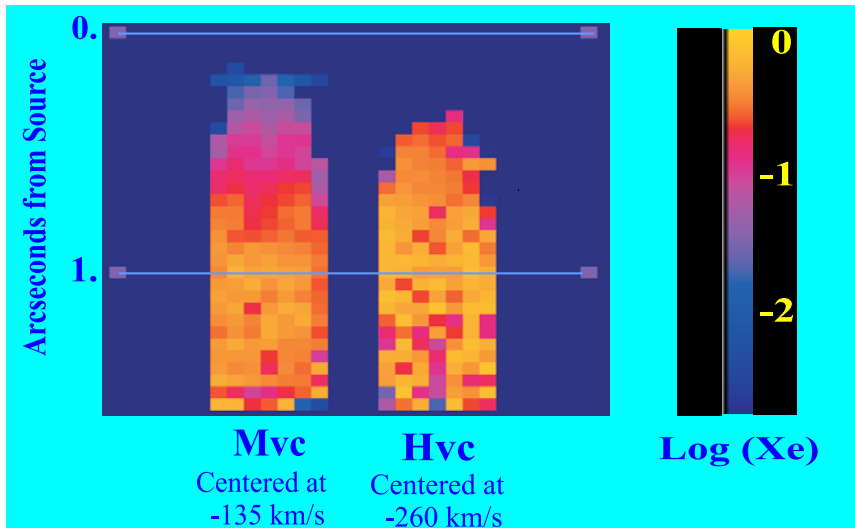


Fig. 3. Same as Fig. 2 but for the ionization fraction, x_e , as derived with the BE technique, in the medium and high velocity bins. Data for the first 0.2'' from the source could not be derived because of the faintness of the [N II] lines.

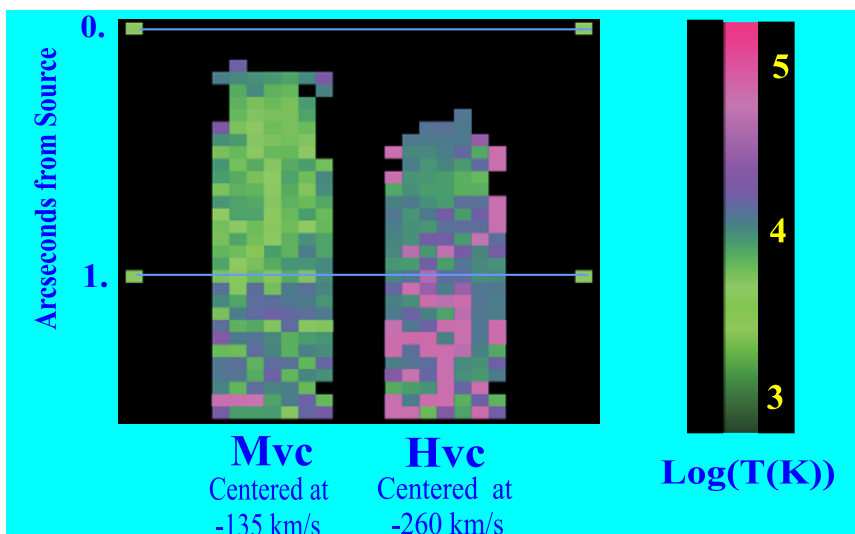


Fig. 4. Same as Fig. 3 but for the temperature T_e . NOTE: THIS FIGURE IS AVAILABLE IN COLOR IN THE ELECTRONIC VERSION OF THIS ARTICLE, OBTAINABLE FROM <http://www.astroscu.unam.mx/~rmaa/>.

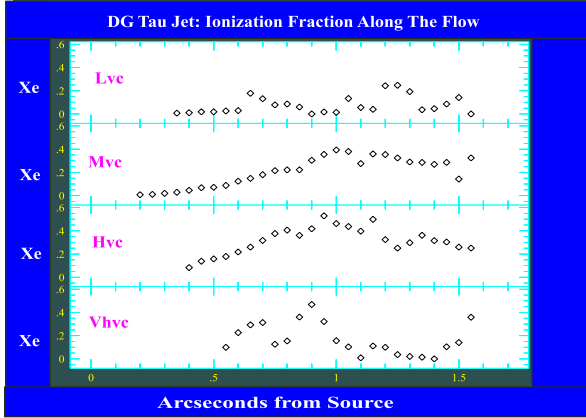


Fig. 5. 1-D projections of the variation of x_e along the DG Tau jet in each velocity bin, obtained averaging over the flow width.

the beam. Finally, the total density n_H (see panel d) decreases from 10^5 to $5 \times 10^4 \text{ cm}^{-3}$ within $1''$, and then steadily falls to 10^4 cm^{-3} at greater distance. These results could indeed be consistent with the ‘flash ionization’ scenario described in § 3. Actually, the variation of x_e and T_e is reminiscent of the one predicted for the cooling region of a steady, radiative oblique shock, located very close to the source. On the other hand, the decay in the total density might reflect the rapid expansion that freezes the ionization. For this flow we also derived estimates of the filling factor and of the mass outflow rate along the beam (panels e and f of Figure 1). Average values turn out to be ~ 0.7 and $1.7 \times 10^{-9} M_\odot \text{ yr}^{-1}$ respectively (see Bacciotti et al. 1999 for a discussion). In the figure, r_{calc} is the jet radius as derived by comparing the calculated and observed fluxes, while r_{obs} is the jet radius measured from the [S II] image.

Encouraged by the findings for HH 30, we then applied the technique to a set of high spatial resolution spectra of the jet from DG Tau, taken in 1999 with STIS aboard *HST*. Seven long-slit spectra were taken keeping the slit parallel to the outflow axis but with steps of $0''.07$ in the transverse direction; each spectrum had a nominal spatial sampling of $0''.05$ and a dispersion of $\sim 25 \text{ km s}^{-1}/\text{pix}$. From the spectra we reconstructed 2D synthetic ‘images’ of the jet in the light of the lines observed ([O I] $\lambda\lambda$ 6300,6363, [N II] $\lambda\lambda$ 6548,6583, [S II] $\lambda\lambda$ 6716,6731, and $H\alpha$), ‘slicing’ the lines in distinct radial velocity intervals (from $+50$ to -400 km s^{-1} , in four bins, each $\sim 125 \text{ km s}^{-1}$ wide). Thus, the derived ‘pictures’ represent the flow in its low, medium, high and very high velocity components (LVC, MVC, HVC,

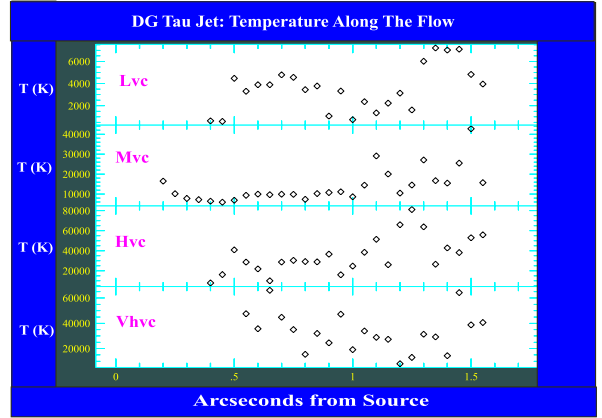


Fig. 6. Same as Fig. 5 but for T_e .

VHVC respectively). We thus obtained a full spatio-kinematical description of the flow at *HST* angular resolution. Multi-wavelength maps of the jet in its first $1''.5$ from the source are presented in this volume in the contribution by Tom Ray (Ray 2002), and a thorough discussion of the jet structure and dynamics can be found in Bacciotti et al. (2000).

Here I will describe the results of the application of the BE technique to the 2D line ratios formed with the reconstructed images shown in (Ray 2002). This extraordinary set of data allowed us to map for the first time the electron density, the ionization fraction and the temperature both *along* and *across* the jet, and in each of its velocity components (Bacciotti et al. 2001). For example, Fig. 2 (see accompanying plate) illustrates the n_e map (‘missing’ data here correspond to positions of high observational uncertainty). The map shows that in this flow, which was already known to be very dense at its base (Solf 1997), n_e is higher in the axial region, and in the more collimated and higher speed components. This finding is interesting, since it is consistent with the predictions of many models of MHD winds (Königl & Pudritz 2000; Shu et al. 1995; Cabrit, Ferreira, & Raga 1999; Lery & Frank 1999).

Figs. 3 and 4 show the derived x_e and T_e maps respectively. Unfortunately for this jet we could not use the bright [O I] λ 6300 line, because a large part of it was out of the imposed spectral range. Thus, we used the [O I] λ 6363 only, which, however, is quite faint. For this reason the results for the LVC and VHVC are poor, and we obtained good bidimensional maps only for the MVC and HVC. Nevertheless, in Figs. 5 and 6 we show for any velocity bin the 1D projections of x_e and T_e along the flow, averaged over the jet width to increase the S/N.

As for the HH 30 jet, we see a gradual increase of the ionization with distance from the star, up to a maximum of about 0.4–0.5, reached at $1''$. The ionization plateau correspond to the interior of a rarefied bubble, inflated by the first internal bow shock, located at $1''.4$ (see Ray 2002). Afterwards x_e decreases again. At the same time the temperature in the MVC rapidly decreases from 2×10^4 K to less than 10^4 K within the first $0''.5$. T_e stays constant at 10^4 K in the bubble, and rises again at the bow shock, apparently reaching $3\text{--}4 \times 10^4$ K (see, however, § 2). Unlike the electron density, neither x_e nor T_e appear to be higher in the axial region. Figures 5 and 6, however, clearly show that both quantities increase with flow velocity and collimation. In the next section I will briefly comment on the above findings; a thorough discussion will appear in Bacciotti et al. (2001).

It is very interesting to note that similar results for the variation of the excitation conditions along the flow have been obtained for the same object and for the jet from RW Aur by Lavalley et al. (2000) and Dougados et al. (2002), who analyse with independent routines, based on the BE technique, data of about $0''.25$ angular resolution. We can thus conclude that in all the four cases in which the base of the jet has been analyzed so far (Th 28, HH 30, DG Tau, and RW Aur) the physical parameters show the same variation with distance from the source. Summarizing, the ionization fraction rapidly rises to reach a plateau, and then slowly decreases following a recombination curve. In the same region the temperature falls by a factor 2–3 and the total density falls by one to two orders of magnitude.

5. DISCUSSION

The results illustrated in the previous sections can serve as useful constraints upon the proposed models of jet formation and evolution. In particular, we have learnt that partial ionization is a dominant feature in the beams of HH jets, and it must be properly taken into account. For example, partial ionization may introduce important differences in the modeling of magnetized jets, due to the effects introduced by collisions between charged particles and neutrals. This point is examined in Safier 1993; Garcia 1999; Garcia et al. 2002. Furthermore, the derived results indicate that the ionization state of the gas is a non-equilibrium one. The ionization appears to be produced at the very beginning of the jet by an unknown mechanism, and then it decouples from the thermal conditions, probably as a consequence of the rapid expansion. At larger distance

from the source, x_e is seen to decline gently on typical recombination time scales. But what is the nature of the ionizing agent? Is this process related to the inflow/outflow engine, or does it depend on the environment? We know that the star itself does not produce enough energetic photons, and in that case x_e would show a different dependence on distance. Several other possibilities are currently being investigated: oblique shocks at the base of the flow (Lavalley et al. 2000), turbulent boundary layers (Binette et al. 1999), ambipolar diffusion heating in the context of steady MHD winds (Safier 1993; Garcia et al. 2002; Shang et al. 2001). A totally different approach would be to consider the production of ionizing photons in reconnection events at the disk/star interface. Magnetic reconnection, a common feature in unsteady magnetic twist models (see Shibata & Kudoh 1999), is supported by the numerous detection of X-ray sources among YSOs (e.g., Glassgold, Feigelson, & Montmerle 2000). It is evident that a full answer to the above questions will require the joint effort of theoreticians and observers; we can hope in this way to add an useful element to realistic models of how the stellar jets are generated in the first place.

I am very grateful to the organizers for the invitation to present this work, and for the travel grant provided. I thank A. Raga, J. Eislöffel, T. Ray, R. Mundt, and U. Locatelli for their contributions to this work. Financial support for this research was provided by ESA.

REFERENCES

- Bacciotti, F., Chiuderi, C., & Oliva, E. 1995 *A&A*, 296, 185
 Bacciotti, F., Hirth, G., & Natta, A. 1996, *A&A*, 310, 309
 Bacciotti, F., & Eislöffel, J. 1999, *A&A*, 342, 717 (BE99)
 Bacciotti, F., Eislöffel, J., & Ray, T. P. 1999, *A&A*, 350, 917
 Bacciotti, F., Mundt, R., Ray, T. P., Eislöffel, J., Solf, J., & Camezind, M., 2000, *ApJ*, 537, L49
 Bacciotti, F., Ray, T. P., Mundt, R., Eislöffel, J., & Solf, J. 2001, in preparation
 Bally, J., & Reipurth, B. 2002, *RevMexAA(SC)*, 13, 1 (this volume)
 Binette, L., Cabrit, S., Raga, A., & Cantó, J. 1999, *A&A*, 346, 260
 Cabrit, S., Ferreira, J., & Raga, A. 1999, *A&A*, 343, L61
 Dougados, C., Cabrit, S., Lavalley-Fouquet, C., & Hersant, F. 2002, *RevMexAA(SC)*, 13, 43 (this volume)
 Downes, T. P., & Ray, T. P. 1999, *A&A* 345, 977
 Garcia, P. 1999, PhD Thesis, Université C. Bernard, Lyon

- Garcia, P., et al. 2002, *RevMexAA(SC)*, 13, 21 (this volume)
- Glassgold, A. E., Feigelson, E. D., & Montmerle, T. 2000, in *Protostars and Planets IV*, eds. V. Mannings, A. P. Boss, & S. S. Russell (Tucson: University of Arizona Press), 429
- Hartigan, P., Morse, J. A., & Raymond, J. 1994, *ApJ*, 436, 125
- Hollenbach, D. J., & McKee, C. F. 1989, *ApJ*, 342, 306
- Königl, A., & Pudritz, R. E. 2000, in *Protostars and Planets IV*, op. cit., 759
- Lavalley-Fouquet, C. 2000, PhD Thesis, Université J. Fourier, Grenoble
- Lavalley-Fouquet, C., Cabrit, S., & Dougados, C. 2000, *A&A*, 356, L41
- Lery, T., & Frank, A. 1999, *ApJ*, 533, 897
- Raga, A. C., Mellema, G., & Lundqvist, P. 1997, *ApJ*, 109, 517
- Ray, T. P. 1996, in the NATO ASI on Solar and Astrophysical MHD Flows, ed. K. Tsinganos (Dordrecht: Kluwer), 539
- Ray, T. P., Mundt, R., Dyson, J. E., Falle, S. A. E. G. & Raga, A. C. 1996, *ApJ*, 468, L103
- Ray, T. P. 2002, *RevMexAA(SC)*, 13, 83 (this volume)
- Safier, P. N. 1993, *ApJ*, 408, 148
- Shang, H., Lizano, S., Glassgold, A. E., & Shu, F. H. 2001, SOMETHING ELSE
- Shibata, K., & Kudoh, T. 1999, in *Star Formation 1999*, ed. T. Nakamoto (Nagoya), 263
- Shu, F. H., Najita, J. R., Ostriker, E., & Shang, H. 1995, *ApJ*, 455, L155
- Shu, F. H., Najita, J. R., Shang, H., & Li, Z.-Y. 2000, in *Protostars and Planets IV*, op. cit., 789
- Solf, J. 1997, in *Herbig-Haro Flows and the Birth of Low Mass Stars*, IAU Symp. 182, eds. B. Reipurth & C. Bertout (Dordrecht: Kluwer), 63